Fast simulation tool for ultraviolet radiation at the earth's surface

Ola Engelsen*
Norwegian Polar Institute, The Polar
 Environmental Centre
N-9296 Tromsø, Norway
E-mail: ola.engelsen@nilu.no

Arve Kylling
Norwegian Institute for Air Research
 (NILU), P.O. Box 100
N-2027 Kjeller, Norway
E-mail: arve.kylling@nilu.no

Abstract. FastRT is a fast, yet accurate, UV simulation tool that computes downward surface UV doses, UV indices, and irradiances in the spectral range 290 to 400 nm with a resolution as small as 0.05 nm. It computes a full UV spectrum within a few milliseconds on a standard PC, and enables the user to convolve the spectrum with user-defined and built-in spectral response functions including the International Commission on Illumination (CIE) erythemal response function used for UV index calculations. The program accounts for the main radiative input parameters, i.e., instrumental characteristics, solar zenith angle, ozone column, aerosol loading, clouds, surface albedo, and surface altitude. FastRT is based on look-up tables of carefully selected entries of atmospheric transmittances and spherical albedos, and exploits the smoothness of these quantities with respect to atmospheric, surface, geometrical, and spectral parameters. An interactive site, http://nadir.nilu.no/~olaeng/fastrt/fastrt.html, enables the public to run the FastRT program with most input options. This page also contains updated information about FastRT and links to freely downloadable source codes and binaries. © *2005 Society of Photo-Optical Instrumentation Engineers.* [DOI: 10.1117/1.1885472]

1 Introduction

Radiation in the ultraviolet (UV) part of the solar spectrum, especially at the shorter UV-B wavelengths (280 to 315 nm), is potentially harmful to a wide range of biological systems, including human health, ecosystems, and agricultural crops. Several radiative transfer models are capable of simulating UV radiation with high accuracy (see, e.g., Weele et al.[1]). However, for applications requiring repetitive computations, such as computations of UV doses, model pseudoinversions, sensitivity studies, operational quality assurance of measured UV spectra, and production of UV maps, such models are generally too computationally demanding. FastRT is a fast, yet accurate UV simulation tool that remedies the preceding computational shortcomings. Other fast models exist, but are limited in their accuracies, range of input parameters, and/or spectral resolution (see Koepke et al.[2] and the references therein). FastRT computes downward surface irradiances in the spectral range from 290 to 400 nm in steps down to 0.05 nm as a function of the most important atmospheric parameters such as solar zenith angle, ozone column, cloud and aerosol optical thicknesses, surface albedo/type, surface altitude, and cloud constellations. It can reconstruct a spectrum within a few milliseconds on a standard PC, which is to our knowledge faster than any other spectral radiative transfer model. Some broadband empirical models[2] are faster than FastRT, but are restricted to fixed dose types (e.g., the UV index). Contrary to techniques based on neu-

ral networks, e.g., STARneuro,[3] which generally suffers from a "black box" nature, proneness to overfitting, and an empirical and elaborate nature of model development, FastRT has a transparent and predictable behavior, uses smooth interpolation schemes such as splines, and has results that are always back-traceable to physical model results. The range of scenarios represented by FastRT is limited only by the size of its look-up table, which can be readily altered or expanded. We concentrated on representing all typical scenarios that would be reasonable guesses for modelers when only common ground data and meteorological information are available. This is generally the case, because detailed "snap-shot" information on optical properties of the atmosphere is rare and can at best be obtained from expensive *in situ* campaigns.

Currently the tool can provide UV irradiance estimates at accuracies similar to most surface UV measurements. FastRT is now a core component of a quality assurance program (http://nadir.nilu.no/~olaeng/CheckUVSpec/CheckUVSpec.html, Engelsen and Kylling[4]) to check and match incoming UV spectra to the European UV database, as well as being an integral part of the Norwegian UV forecasting system.

In this paper, we first describe the FastRT simulation tool (Sec. 2). Next, we assess the uncertainties of the surface irradiances produced by FastRT, and the computational speed of the FastRT program (Sec. 3).

2 Method

FastRT computes surface irradiances by interpolations and extrapolations of atmospheric transmittances and reflectances stored in look-up tables (LUTs). The transmittances

---

and reflectances pertain to carefully selected wavelengths and scenarios from which other conditions can be deduced with optimal accuracy. In the following, we first describe the contents of the LUTs (Sec. 2.1), followed by an outline of the processing of the content of the LUTs (Sec. 2.2). Further information on the processing details is available within the source code, which is freely available on the Internet at http://nadir.nilu.no/~olaeng/fastrt/fastrt.html

2.1 LUTs

LUTs were computed using the freely available, yet rigorous and accurate LibRadtran atmospheric radiative transfer software package, version 0.99 (http://www.libradtran.org). LibRadtran has a number of radiative transfer equation solvers, including the multistream discrete ordinates radiative transfer (DISORT) equation solver by Stamnes et al.[5] The computations for the LUTs were made using DISORT including the pseudospherical approximation (SDISORT) by Dahlback and Stamnes[6] to ensure high levels of accuracy even for low solar elevations.

The LUTs enclosed with the FastRT were computed assuming the following fixed atmospheric and surface conditions as well as modeling options:

1. Air Force Geophysics Laboratory (AFGL) U.S. standard atmosphere.[7]
2. The solar ultraviolet spectral irradiance monitor (SUSIM) extraterrestrial solar spectrum measured[8] onboard the Space Shuttle during the ATLAS 3 mission in November 1994.
3. Aerosol Ångström coefficients $\alpha = 1.3$, where the aerosol optical depth$= \beta \lambda^{-\alpha}$, where λ is the wavelength in micrometers. This α value is close to the mean for remote/urban locations, and is not unlikely for desert, coastal, oceanic, and high-altitude surroundings.[9]
4. Homogeneous water clouds of user-specified density at 2 to 7 km above ground with a droplet radius of 7.2 μm, similar to alto-stratus clouds.[10] The vertical location and the thickness of the cloud have a modest effect in UV-A [Fig. 1(a)], but have a much larger effect in UV-B, where absorption and scattering between cloud droplets and ozone/air molecules is much stronger [Fig. 1(b)]. When a cloud droplet radius other than 7.2 μm is present, the irradiance error is less than 15% for water clouds (i.e., droplet effective radii in the range 3 to 20 μm, see Ref. 10). However, information on cloud vertical distribution and droplet radii is not usually available. The assumed cloud scenario is a reasonable choice.
5. Temperature-dependent ozone absorption cross section from Molina and Molina.[11]
6. Spring/summer aerosol profile.[10]
7. Rural tropospheric aerosol (from MODTRAN 3, see Abreu and Anderson[12]).
8. Stratospheric aerosol: background conditions (from MODTRAN 3).
9. Surface types: spectral surface albedos for 12 surface types were obtained from Feister and Grewe,[13] and another 6 surface types were provided by Blumthaler and Ambach.[14] Alternatively, the user can specify arbitrary surface albedo values [0 to 1].
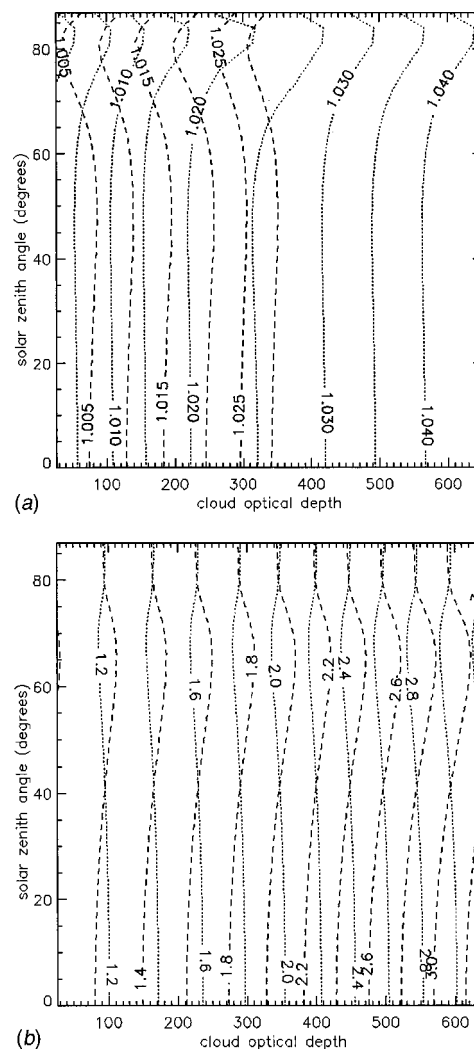

(a)

(b)

Fig. 1 Contour plots of the ratios of (a) 360- and (b) 305-nm irradiances produced by LibRadtran for a 1-km-thick cloud just above ground (dashed) and at an 8- to 9-km altitude (dotted) with respect to the cloud assumed in FastRT (2 to 7 km). The results are shown in terms of cloud optical depth and solar zenith angle. The plots pertain to a clear atmosphere with an ozone column of 340 Dobson units (DU) over a nonreflecting surface at sea level. The cloud optical thickness is the cloud liquid water column times 650/4000.

10. Delta-M approximation for forward aerosol scattering.
11. Number of streams: 12.
12. Number of atmospheric layers: 49.

The LUTs contain spectral transmittances (i.e., the downward flux at the surface divided by the extraterrestrial solar flux when there is no reflection from the surface) and atmospheric spherical albedos (i.e., downward flux divided by a hypothetical diffuse upward flux from a black surface). The LUT entries are stored in small files and represent a wide variety of conditions (Tables 1 and 2). Their filenames contain unique codes that identify the underlying optical properties of the atmosphere. FastRT extracts the required LUT files by opening named files. The program thus exploits the computer operating system's own efficient file search utility.

Table 1 Variable parameters for tabulated atmospheric transmittances.

Parameter	Tabular values
Spectral wavelengths (nm)	116 wavelengths in [290,400]
Solar zenith angle (deg.)	[0,87], step 3
Total ozone (DU)	[100 to 600], step 20
Surface altitude (km)	0, 3, and 6
Cloud liquid water column (g m^{-2})	0, 160, 240, 400, 560, 1040, 1640, 2320, 4000

2.2 LUT Entries and Processing

Atmospheric transmittances at 116 spectral locations were optimally distributed so that spline interpolations could most accurately reconstruct the real spectral transmittances at arbitrary wavelengths in the range 290 to 400 nm (Fig. 2). "Black surface" irradiances are then computed by multiplying the transmittances with an extraterrestrial solar spectrum, corrected for the earth-to-sun distance. The output spectral resolution is thus only limited by the spectral resolution of the ATLAS 3 extraterrestrial solar spectrum,[8] which is 0.05 nm. The cloud densities were selected so that spline interpolation would yield a good approximation (Fig. 3). Transmittances as a function of total ozone and solar zenith angles were also approximated quite accurately by spline interpolations from a regular grid of 20 DU and 3 deg., respectively. Transmittances under various aerosol loadings (Ångström β) are, however, estimated by multiplying an aerosol modification factor with a clear atmospheric (Ångström β=0.02) transmittance. The aerosol modification factors were computed from second-order polynomials (Fig. 4). The polynomial coefficients were relatively insensitive to wavelengths, total ozone, and solar zenith angles, and only a coarse grid of coefficients was required. The coefficients were optimally fitted to transmittances simulated by LibRadtran. In these simulations, the aerosol profile shape was retained, but scaled to the correct aerosol optical depth. In case the user specifies atmospheric visibility (R_m in kilometers) instead of the aerosol Ångström coefficient v, the latter is computed using a formula by Iqbal[15]: $\beta = 0.55^\alpha[3.912/R_m \text{ km} -0.01162][0.02472(R_m \text{ km}-5)+1.132]$, where $\alpha = 1.3$ is the aerosol Ångström α coefficient.

The atmospheric transmittance at the user-specified surface altitude is estimated from a second-order polynomial which is fitted to atmospheric transmittances at 0, 3, and 6 km altitudes.

For a reflecting surface, the downward surface irradiance E is computed from radiation transmitted through the atmosphere in addition to contributions from an infinite series of successive Lambertian reflections back and forth between the surface and the atmosphere, i.e.,

$$E = E_0 T(1 + AS + A^2 S^2 + A^3 S^3 + \cdots) = E_0 T/(1-AS), \quad (1)$$

where E_0 is the extraterrestrial irradiance, T is the transmittance of the atmosphere, S is the spherical albedo of the atmosphere when illuminated from below by isotropic radiation, and A is the surface albedo. This scheme for radiative coupling of the surface and the atmosphere is similar to that employed for some two-stream adding-doubling (e.g., Hansen and Travis[16]) and successive orders of scattering (e.g., Vermote et al.[17]) radiative transfer models. The simulated surface irradiances (E) are much less sensitive to errors in atmospheric spherical albedos (S) than to errors in atmospheric transmittances (T), and the significance of errors in atmospheric spherical albedos (S) decreases with diminishing surface albedo (A). Furthermore, the influence of stratospheric ozone and solar zenith angles on atmospheric spherical albedos (S) could be disregarded. The atmospheric spherical albedos were tabulated at wavelength intervals of 10 nm and only in terms of altitude and cloud thickness. Spline interpolations to the correct wavelength, altitude, and cloud thickness are done. The effect of ozone and aerosol loadings were estimated by modification factors computed from second-order polynomials with tabulated coefficients expanded around an ozone column of 300 DU and an aerosol Ångström β of 0.02. The atmospheric spherical albedos are exact for those ozone and aerosol conditions.

FastRT has four cloud options: no clouds, homogeneous clouds, "scattered clouds," and "broken clouds." The latter two constitute two separate ways to account for horizontally inhomogeneous clouds. For the FastRT input option "scattered clouds," the computed surface irradiance (E) is a linear combination of the irradiances under a homogeneous cloud cover (E_{cloud}) and that under cloudless conditions ($E_{\text{cloudless}}$), i.e., $E = \text{CF} \times E_{\text{cloud}} + (1-\text{CF})E_{\text{nocloud}}$, where CF is the cloud fraction. For the option "broken clouds," we assume that downward radiation is transmitted as if only a clear atmosphere was present, but at the surface, all radiation is reflected between the cloudy atmosphere and the surface until absorbed. In other words, the downward surface irradiance (E) is computed from Eq. (1), except that

Table 2 Variable parameters for tabulated atmospheric spherical albedos.

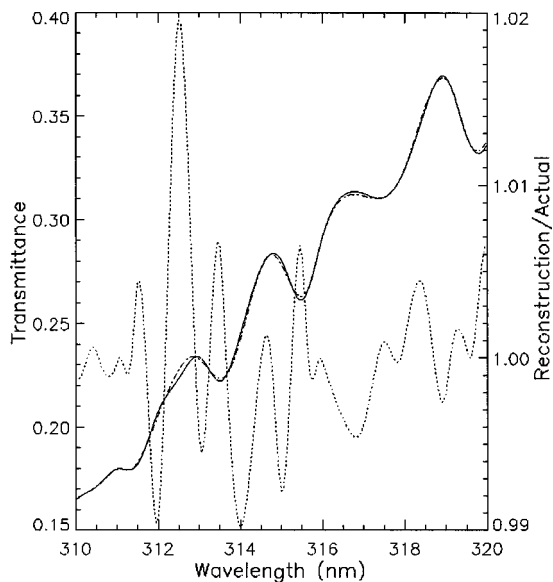| Parameter	Tabular values
Spectral wavelengths (nm)	[290,400], step 10
Surface altitude (km)	0, 3, and 6
Cloud liquid water column (g m^{-2})	0, 160, 240, 400, 560, 1040, 1640, 2320, 4000

Fig. 2 Transmittance of a clear atmosphere at a solar zenith angle of 40 deg., ozone column of 300 DU at sea level. The dashed line is the reconstruction of the actual (solid line), and illustrates the performance of spline interpolations. The dotted line is the ratio of the reconstructed transmittance to the actual transmittance computed by LibRadtran.

Fig. 4 Atmospheric transmittance with respect to Ångström β at a solar zenith angle of 45 deg., with an ozone column of 300 DU at sea level. The dashed line is the reconstruction of the actual (solid line). The dotted line is the ratio of the two.

only the atmospheric spherical albedo (S) pertains to a cloudy atmosphere. This scenario represents an extreme condition where surface radiation is greatly enhanced; up to five times when trapped between a snow surface and a thick cloudy atmosphere.

2.3 UV Action Spectra, Dose Rates, and Daily Doses

An action spectrum describes the relative effectiveness of energy at different wavelengths in producing a particular biological response. It is used as a "weighting factor" for the UV spectrum to find the actual biologically effective

Fig. 3 Transmittance of an atmosphere containing a 4-km-thick cloud as function of liquid water columns. The cloud droplet size is 7.2 μm, the ozone column is 300 DU, and the solar zenith angle is 45 deg. The dashed line is the reconstruction of the actual (solid line). The dotted line is the ratio of the two.
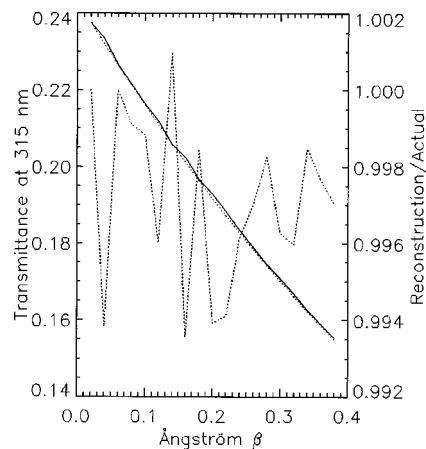
dose rate (BED) for a given effect. The total dose rate (consistent with milliwatts per meter squared) is found by integrating the product of UV irradiance and the action spectrum values over the wavelength range from 290 to 400 nm. A daily dose is the dose rate integrated over a 24-h day (=86,400 s). The daily dose has units consistent with joules per meter squared. Currently, FastRT can readily compute more than 20 different types of biologically effective doses/dose rates, including the widely used International Commission on Illumination (CIE) erythema,[18] UV-B (uniform 290 to 315 nm), and SCUP-H.[19] A complete and updated list of biologically effective dose types along with corresponding references are available in the FastRT documentation (http://nadir.nilu.no/~olaeng/fastrt/README.html).

2.4 User Interfaces

The FastRT program can be run through a graphical user interface on a Web browser, or from the operating system prompt. The latter is faster and is more suitable for multiple runs and inclusion in computer scripts. The interactive version found at http://nadir.nilu.no/~olaeng/fastrt/fastrt.html enables the public to run the FastRT program with most input options. This page also contains updated information about FastRT and links to freely downloadable source codes and binaries. The most important input parameters are user controlled, e.g., ozone column, instrumental spectral response function, aerosol optical depth, cloud liquid water column, and surface albedo/type.

3 Results

3.1 Computational Speed

The computational speed of the FastRT program depends on the number of irradiances to be calculated, the width of the spectral response function, and the type of scenario to be simulated. The test results presented here were obtained from a low-end standard PC (2.5-GHz Pentium 4) running the Red Hat Linux 9.0 operating system with a GNOME user interface. Spectra were computed more efficiently than single irradiances. Simulation of a single monochromatic clear sky irradiance at 300 nm took 15 ms, whereas com-

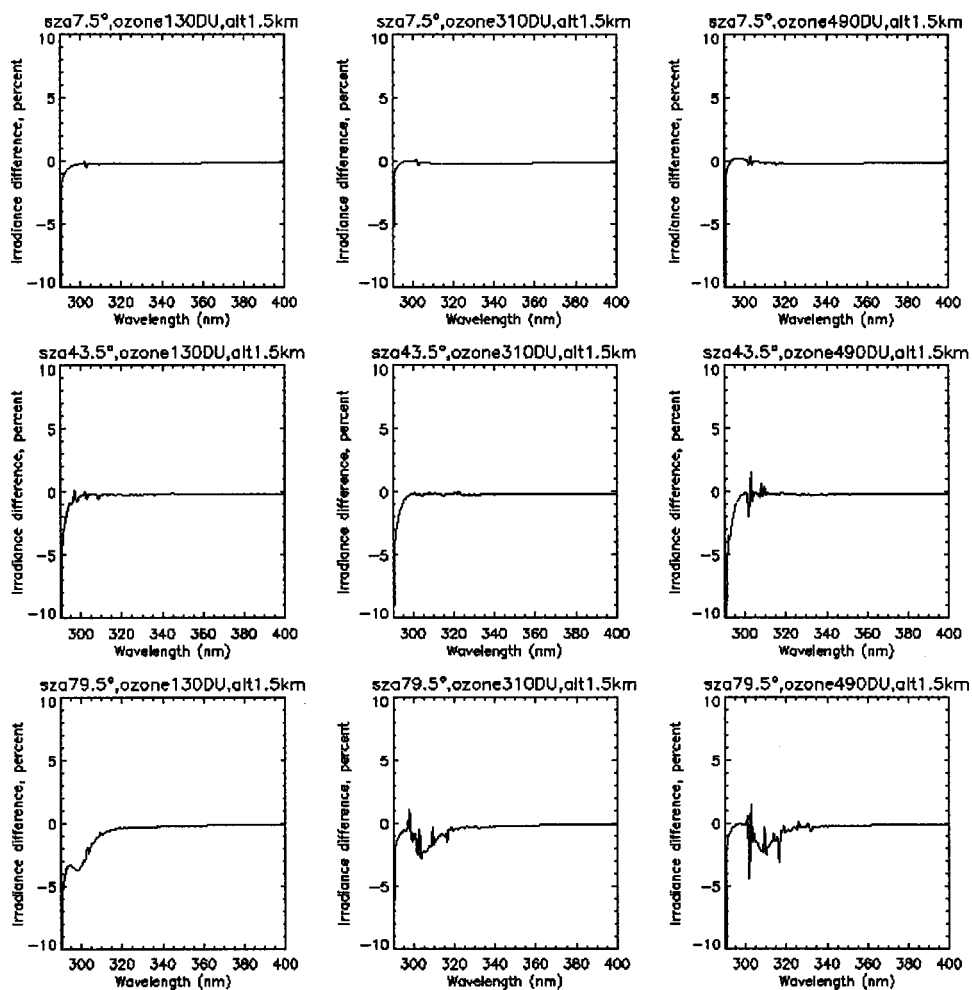**Table 3** Variable parameters for generation of test cases.

Parameter	Test values
Solar zenith angle (deg.)	4.5, 22.5, 40.5, 58.5, 76.5
Total ozone (DU)	150, 250, 350, 450, 550
Aerosol Ångström β	0.1, 0.175, 0.25, 0.325, 0.4
Surface albedo	0.1, 0.3, 0.5, 0.7, 0.9
Surface altitude (km)	0.5, 1.5, 2.5, 3.5, 4.5
Cloud liquid water column (g m^{-2})	200, 480, 800, 1360, 3160

Table 4 Absolute errors in percent [mean $\pm 2\sigma$ (maximum)] of FastRT with respect to LibRadtran results for irradiances at wavelengths of 305 and 355 nm as well as for the CIE erythemally weighted dose rate[17]/UV index.[20] Errors for clear, turbid (aerosol loaded), and cloudy atmospheres are shown.

	305 nm	355 nm	CIE dose rate/ UV index
Clear	0.8±1.7 (4.1)	0.0±0.1 (0.1)	0.2±0.3 (0.7)
Cloudless turbid	2.0±5.9 (19.3)	0.7±1.2 (2.9)	0.8±2.4 (13.0)
Cloudy	6.8±12.0 (33.7)	2.5±2.2 (5.2)	4.1±6.7 (30.6)

putation of 111 monochromatic irradiances in the range 290 to 400 nm at equidistant 1-nm steps was accomplished within 18 ms. Such a spectrum forms the basis for UV dose rates and UV indices produced by FastRT. Cloudy, turbid, above sea level, and reflective ground conditions require more interpolations and processing and are somewhat slower to simulate, sometimes up to 160 ms. Irradiances with a spectral response function influences the computation time considerably, because convolutions are then evaluated at a 0.05-nm resolution. In the UV spectral region, this elaborate process is necessary especially for narrowband irradiances to account properly for the Fraunhofer lines of the extraterrestrial solar spectrum, as well as the rapid spectral fluctuations in the ozone absorption cross sections. By extreme, the 345-nm irradiance with a triangular spectral response function of 55 nm (full width at half

Fig. 5 Figures above show the percentage difference of the surface irradiance spectra for a clear sky scenario generated by the FastRT model and the LibRadtran model with respect to the latter. The titles indicate solar zenith angles (sza) in degrees, total ozone columns (ozone) in Dobson units, and surface altitude (alt) in kilometers. The plots illustrate the expected worst-case scenarios for clear sky, i.e., wavelengths, total ozone columns, solar zenith angles, and surface altitudes are all centered between the tabular entries.

maximum), may take as much as 164 ms to compute. A full spectrum ranging from 290 to 400 nm in 0.5-nm steps and a triangular spectral response function of 0.6 nm (similar to Bentham type spectroradiometers) took 117 ms to reproduce for typical cloudless conditions. By contrast, the LibRadtran program produced the same result after 19 s, i.e., ca. 160 times later. However, DISORT has been shown to be a very efficient radiative transfer equation solver, particularly for optically thick (e.g., cloudy) atmospheres.[5] FastRT may thus perform even better in comparison to many other rigorous and accurate radiative transfer models.

For users with even more stringent computational requirements, several times faster versions of FastRT with simpler, but less accurate, interpolation schemes are available from the lead author on request.

3.2 Error Analysis

We compared FastRT (version 2) simulations to results obtained from LibRadtran for a large number of test scenarios covering the full range of the major input parameters, i.e., solar zenith angle, ozone column, visibility, surface altitude, surface albedo, and cloud liquid water columns (Tables 3 and 4). All scenarios selected for these tests were centred between tabular entries where we would expect the largest deviations. The more similar the atmospheric scenarios are to those represented within tabular entries of the FastRT source code (Tables 1 and 2), the better the agreement between LibRadtran and FastRT. When the scenarios and wavelengths match, the programs produce exactly the same results.

In general, the FastRT program produces UV irradiances and doses with uncertainties comparable to those of UV measurements, provided all model input parameters are known. Due to errors in radiometric calibration, cosine error, wavelength misalignment, noise, etc., even high-quality UV measurements have uncertainties ($\pm 2\sigma$) of about 6% in the UV-A and for CIE dose rates and 13% at a 300-nm wavelength at a 60-deg. solar zenith angle.[21] These numbers form the standard for our following analysis.

1. For nearly clear sky scenarios (i.e., aerosol Ångström $\beta=0.02$), the errors were always less than 4% and mostly negligible ($\ll 6\%$) for all UV irradiances and dose rates. The errors can be somewhat larger for wavelengths below 300 nm (Fig. 5).

2. For cloudless, but turbid, aerosol loaded atmospheres (aerosol Ångström $\beta>0.02$), the maximum error was 19% and 13% for the 305-nm irradiances and the CIE dose rates, respectively. However, at least 95% of the FastRT simulations agreed well with (i.e., within 8% of) corresponding results from LibRadtran. For UV-A (355 nm) the agreement was quite good ($<6\%$) for all tests. The largest FastRT errors occurred in UVB with high aerosol loadings at high altitudes (Fig. 6).

3. For cloudy scenarios, the errors were higher than for cloudless atmospheres. The maximum errors could occasionally exceed 30%, but 67% ($\pm 1\sigma$) of the test errors were within the uncertainty bounds expected for measurements of UV-B irradiances and CIE doses. For UV-A (355 nm), the errors were better than the expected UV measurement uncertainties ($<6\%$) for all tests. The largest errors occurred in the
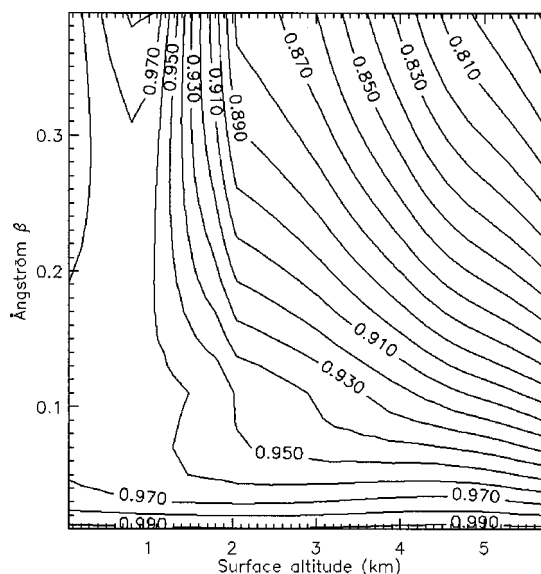

Fig. 6 Contour plot of the ratio between 305-nm irradiances produced by FastRT to those simulated by LibRadtran as a function of aerosol Ångström coefficient β and surface altitude under identical cloudless conditions. The plot pertains to a solar zenith angle of 76.5 deg., an ozone column of 450 DU, and a surface albedo of 0.9.

UV-B for thick clouds, particularly in combination with a high surface albedo (Fig. 7). Note that rather large variabilities in optical properties of clouds can occur, constituting a huge uncertainty in UV simulations. The effect of clouds on surface radiation is generally much larger than that of aerosols. FastRT thus ignores the effect of aerosols when clouds are present.

4. For the tests done within the measured UV spectrum diagnosis program CheckUVSpec (not shown here) (see http://nadir.nilu.no/~olaeng/CheckUVSpec/CheckUVSpec.html and Ref. 4), the FastRT errors did not exceed 1%, and were thus negligible ($\ll 6\%$).

In the error analysis we used LibRadtran as a benchmark. LibRadtran has been shown to agree well with both other
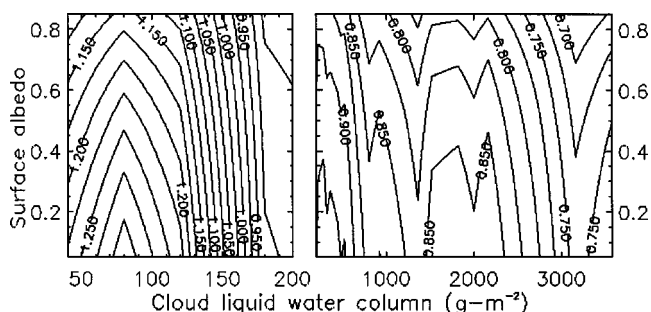

Fig. 7 Contour plots of the ratio between 305-nm irradiances produced by FastRT to those simulated by LibRadtran as a function of surface albedo and cloud liquid water column. The plots are shown for a surface altitude of 4.5 km, a solar zenith angle of 76.5 deg., and an ozone column of 550 DU. The left and right panels show different sections of the x-axis.

models and measurements.[1,22–24] Note that all fixed input parameters of LibRadtran were the same as when the LUTs were generated.

4 Discussion and Conclusion

The FastRT program can simulate a UV spectrum within a few milliseconds, which is at least hundreds of times faster than the most rigorous and accurate models based on a numerical solution of the radiative transfer equation. The exact computation time depends somewhat on the input parameters.

The uncertainties of the FastRT output are, in general, better than that of high-quality UV measurements, provided the atmospheric input parameters are known. We expect no outliers, i.e., occasional extremely large errors. For the conditions covered by FastRT, the largest deviations from LibRadtran occur for wavelengths below 300 nm and with thick clouds present. However, surface instruments also have largest uncertainties below 300 nm, and clouds are the most difficult atmospheric scattering constituents to determine precisely, even during rigorous measurement campaigns.

Applications of FastRT are diverse, ranging from operational simulation of UV doses to detailed reproduction of real UV measurements. The program is easy to use, and accepts atmospheric and surface input parameters at a detail level suitable for many users. Other fast models are generally more limited in their scope of applications and input parameters. FastRT is freely available on the Internet, and can also be obtained from the lead author on request.

References

1. M. van Weele, T. J. Martin, M. Blumthaler, C. Brogniez, P. N. den Outer, O. Engelsen, J. Lenoble, G. Pfister, A. Ruggaber, B. Walravens, P. Weihs, H. Dieter, B. Gardiner, D. Gillotay, A. Kylling, B. Mayer, G. Seckmeyer, and W. Wauben, "From model intercomparison towards benchmark UV spectra for six real atmospheric cases," *J. Geophys. Res.* **105**(D4), 4915–4925 (2000).
2. P. Koepke, A. Bais, D. Balis, M. Buchwitz, H. D. Backer, X. D. Cabo, P. Eckert, P. Eriksen, D. Gillotay, A. Heikkilä, T. Koskela, B. Lapeta, Z. Litynska, J. Lorente, B. Mayer, A. Renaudl, A. Ruggaber, G. Schauberger, G. Seckmeyer, P. Seifert, A. Schmalwieser, H. Schwander, K. Vanicek, and M. Weber, "Comparison of models for UV index calculations," *Photochem. Photobiol.* **67**(6), 657–662 (1998).
3. H. Schwander, A. Kaifel, A. Ruggaber, and P. Koepke, "Spectral radiative transfer modelling with minimized computation time using neural network technique," *Appl. Opt.* **40**(3), 331–335 (2001).
4. O. Engelsen and A. Kylling, "Fast simulation tool for UV radiation and diagnosis of measured UV spectra," in *Ultraviolet Ground and Space-based Measurements, Models and Effects III*, J. R. Slusser, J. R. Herman, and W. Gao, Eds., *Proc. SPIE* **5156**, 409–419 (2003).
5. K. Stamnes, S. C. Tsay, W. Wiscombe, and K. Jayaweera, "A numerically stable algorithm for discrete ordinate method radiative transfer in multiple scattering and emitting layered media," *Appl. Opt.* **27**, 2502–2509 (1988).
6. A. Dahlback and K. Stamnes, "A new spherical model for computing the radiation field available for photolysis and heating at twilight," *Planet. Space Sci.* **39**, 671–683 (1991).
7. G. P. Anderson, S. A. Clough, F. X. Kneizys, J. H. Chetwynd, and E. P. Shettle, "AFGL atmospheric constituent profiles (0–120 km)," Tech. Rep. AFGL-TR-86-0110, Air Force Geophys. Lab., Hascom Air Force Base, MA (1986).
8. M. E. Van Hoosier, "The ATLAS-3 solar spectrum," Naval Research Laboratory, Washington, DC (1996); available via anonymous ftp (ftp://susim.nrl.navy.mil/pub/atlas3).
9. S. Gonzi, D. Baumgartner, and E. Putz, "Aerosol climatology and optical properties of key aerosol types observed in Europe," IGAM/UG Technical Report for EU (2002); available at http://www.muk.uni-hannover.de/~martin/results/deliverables/1.5/b.pdf.
10. E. P. Shettle, "Models of aerosols, clouds and precipitation for atmospheric propagation studies," in *Atmospheric Propagation in the UV, Visible, IR and MM-Region and Related System Aspects, AGARD Conf. Proc.*, 15.1–15.13 (1989).
11. L. T. Molina and M. J. Molina, "Absolute absorption cross-sections of ozone in the 185–310 nm wavelength range," *J. Geophys. Res.* **91**, 14501–14508 (1986).
12. L. W. Abreu and G. P. Anderson, "The MODTRAN 2/3 Report and LOWTRAN 7 Model," Prepared by Ontar Corporation for PL/GPOS (1996).
13. U. Feister and R. Grewe, "Spectral albedo measurements in the UV and visible region over different types of surfaces," *Photochem. Photobiol.* **62**, 736–744 (1995).
14. M. Blumthaler and W. Ambach, "Solar UVB-Albedo of various surfaces," *Photochem. Photobiol.* **48**(1), 85–88 (1988).
15. M. Iqbal, *An Introduction to Solar Radiation*, Academic, San Diego, CA (1983).
16. J. E. Hansen and L. D. Travis, "Light scattering in planetary atmospheres," *Space Sci. Rev.* **16**, 527–610 (1974).
17. E. Vermote, D. Tanre, J. L. Deuze, M. Herman, and J. J. Morcrette, "Second simulation of the satellite signal in the solar spectrum: an overview," *IEEE Trans. Geosci. Remote Sens.* **35**, 675–686 (1997); ftp://loaser.univ-lille1.fr/6S.
18. A. F. McKinlay and B. L. Diffey, "A reference action spectrum for ultraviolet induced erythema in human skin," *CIE J.* **6**(1), 17–22 (1987).
19. F. R. de Gruijl and J. C. van der Leun, "Estimate of the wavelength dependency of ultraviolet carcinogenesis in humans and its relevance to the risk assessment of a stratospheric ozone depletion," *Health Phys.* **67**, 319–325 (1994).
20. World Meteorological Organization (WMO), "Report of the WMO-WHO Meeting of Experts on Standardization of UV indices and their dissemination to the public," WMO Rep. 127, Les Diablerets, Switzerland (1997).
21. G. Bernhard and G. Seckmeyer, "Uncertainty of measurements of spectral solar UV irradiance," *J. Geophys. Res.* **104**(D12), 14321–14345 (1999).
22. A. Kylling, T. Danielsen, M. Blumthaler, J. Schreder, and B. Johnsen, "Twilight tropospheric and stratospheric photodissociation rates derived from balloon borne radiation measurements," *Atmos. Chem. Phys.* **3**, 377–385 (2003).
23. A. Hofzumahaus, A. Kraus, A. Kylling, and C. Zerefos, "Solar actinic radiation (280–420 nm) in the cloud-free troposphere between ground and 12 km altitude: measurements and model results," *J. Geophys. Res.* **107**, PAU 6-1–PAU 6–11 (2002).
24. A. Kylling, A. F. Bais, M. Blumthaler, J. Schreder, C. S. Zerefos, and E. Kosmidis, "The effect of aerosols on solar UV irradiances during the Photochemical Activity and Solar Ultraviolet Radiation campaign," *J. Geophys. Res.* **103**, 26051–26060 (1998).

Ola Engelsen is a senior scientist in atmospheric physics at Norwegian Institute of Air Research (NILU) in Tromsø. His research interests include radiative transfer modeling, UV radiation and remote sensing. He received his PhD in applied physics from the University of Tromsø, Norway.

Arve Kylling received his PhD in atmospheric physics from the University of Alaska, Fairbanks. Until recently he was a senior research scientist at the Norwegian Institute for Air Research (NILU). He has worked with radiative transfer in the Earth's atmosphere since 1988. Together with Dr. B. Mayer, the German Aerospace Center (DLR), he is developing a much used radiative transfer model. Presently he works on cancer radiation therapy at the Trondheim University Hospital, Norway.